Metasurface-Based Dual-Band Circularly Polarized Antenna for X-Band Applications

Abdul Majeed, Yejun He* and Shahid Ullah
State Key Laboratory of Radio Frequency Heterogeneous Integration
Sino-British Antennas and Propagation Joint Laboratory of MOST
Guangdong Engineering Research Center of Base Station Antennas and Propagation
Shenzhen Key Laboratory of Antennas and Propagation
College of Electronics and Information Engineering, Shenzhen University, 518060, China
Email: heyejun@126.com*

2025 International Conference on Microwave and Millimeter Wave Technology (ICMMT) | 979-8-3315-2573-6/25/$31.00 ©2025 IEEE | DOI: 10.1109/ICMMT65948.2025.11188814

***Abstract*—This paper presents metasurface (MS)-based dual-band circularly polarized (CP) antenna. To improve the impedance bandwidth (IBW) and perform linearly polarized (LP) to circularly polarized conversion, a 50 Ω coplanar waveguide (CPW) microstrip-line-fed termination with an open radial stub is employed. With an overall size of 40 mm × 40 mm × 1.658 mm, the proposed antenna array produced an impedance bandwidth ($|S_{11}| \leq -$ 10 dB) of 7.88–9.03 GHz and 9.36–9.46 GHz with an axial ratio bandwidth of 8.74–8.87 GHz and 9.35–9.44 GHz. Also, it achieves a 90% radiation efficiency and yields broadside left-handed circularly polarized (LHCP) and right-handed circularly polarized (RHCP) radiation with a gain of 4.9 dBi. Additionally, it achieves a peak gain of 8.6 dBi at 8.2 GHz. The proposed antenna is a potential candidate for X-band applications.**

***Index Terms*—circularly polarized, CPW, metasurface, axial ratio, gain.**

I. Introduction

Circularly polarized (CP) antennas provide a highly flexible transmitter/receiver orientation for reliable and stable signal transmission. Due to their ability to mitigate multipath fading, reduce Faraday rotation, and provide immunity to polarization mismatching between transmitting and receiving antennas, they are widely used in wireless applications [1]. Recently, there has been a lot of interest in metasurface (MS) antennas due to their many advantages over conventional patch antennas, such as their wide bandwidth and high gain [2]. The MS antenna can achieve CP radiation by modifying the feeding structure to supply the orthotropic current source. At a 3-dB axial ratio (AR) bandwidth of 5.6%, the first LP-to-CP conversion [3] using a single dipole on an artificial ground plane was accomplished. The broadband CP radiation was excited using a single Z-shaped feeding slot, as detailed in [4]. The radiation element had a 4 × 4 mushroom structure to generate wide bandwidth and high gain [4]. The realized gain is between 5.1 and 8.1 dBi, and the 3 dB ARBW is 28%. In [5], the CP radiation with an average gain of 4.33 dBi and a IBW of 11.6% is generated by feeding a 45 square ring elements array through a cross slot. A pattern-reconfigurable annular slot-augmented circular patch antenna with switchable broadside and conical CP beams was reported [6]. Cutting slots or adding strips to MS is another method of producing CP radiation. A wideband dual-mode patch antenna with compact CPW feeding network for pattern diversity application was proposed [7]. These antennas, however, have relatively large antenna height because their primary radiating elements are placed above the metasurfaces.

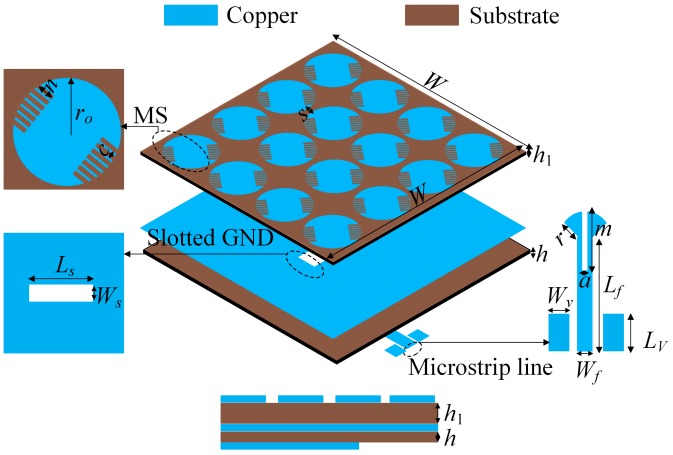

Fig. 1. Depolyed view of the proposed metasurface antenna.

This work presents a metasurface-based circularly polarized antenna. An open circuit radial stub termination with a CPW microstrip-fed line is used to enhance impedance bandwidth and achieve LP-to-CP conversion. The proposed antenna has been designed specifically for X-band applications. To summarize, the proposed antenna is easy to use in the feeding network, has a simple design, and has the appropriate gain.

II. Metasurface-Based CP Antenna Design

Fig. 1 shows the deployed view of the proposed MS-based CP antenna, which has dimensions of 40 mm × 40 mm × 1.658 mm. As shown in Fig. 1, the proposed antenna consists of two substrate layers. The 4 × 4 double-headed comb-shaped MS array operates as a radiation structure on top of the upper substrate. The ground plane of the MS array is inserted between two substrates with thicknesses of h_1 and h. The two substrate layers are Rogers RO4003C, with a thickness of 1.6 mm for h_1 and 0.508 mm for h. In this work, a feeding slot with length L_s and width W_s is etched centrally

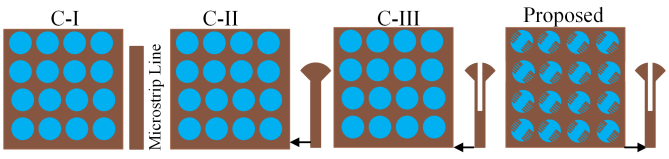

Fig. 2. Evaluation steps of 4×4 array antenna with microstrip feed line.

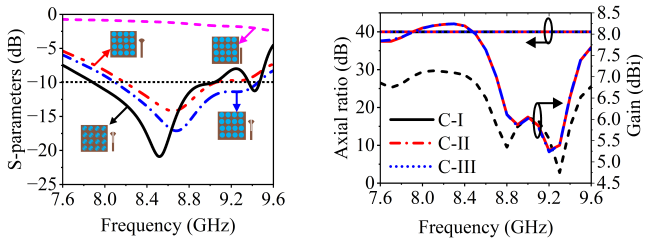

(a) (b)

Fig. 3. Simulated results of different cases (a) S-parameters (dB) (b) Axial ratio (dB) with gain (dBi).

TABLE I
DIMENSIONS OF THE PROPOSED ANTENNA

Parameters	Values (mm)	Parameters	Values (mm)
W	40.0	s	4.40
W_s	2.00	L_s	14.0
n	1.30	r_o	4.0
c	0.30	a	0.40
r	2.6	m	9.90
W_f	1.13	L_f	20.57
W_v	4.60	L_v	6.00

on the ground plane of the MS, in contrast to the plane wave incident feeding. To modify the impedance matching, a 50 Ω microstrip line with an open-circuit radial stub termination is printed on the bottom of the lower substrate layer as a feeding line, as illustrated in Fig. 1. The side view of the feeding structure shows that the radius of the radial stub is r. Following the optimization procedure, Table I presents the optimized parameters.

A. Evaluation Process and CP conversion

This section details the evaluation process of the proposed MS antenna and linear to circular polarization conversion approach. The stepwise design cases are displayed in Fig. 2. Case 1 introduces an array of 4 × 4 circular radiators with a 50 Ω microstrip feed line (represented by C-I). In case 2 (C-II), a microstrip line was top-loaded with a virtual radial stub termination to improve the impedance bandwidth. In case III, the radial stub microstrip line was loaded with an open rectangular slot. In the final step (proposed), dual-band CP performance was achieved by inserting a 45° rectangular slot into a circular radiator. The CST Microwave Studio 2022 is used to complete the design and analysis steps of this work. The S-parameters and axial ratio stepwise simulated results with the gain (dBi) are displayed in Fig. 3. As Fig. 3(a) shows, the C-I is not an antenna due to poor impedance matching

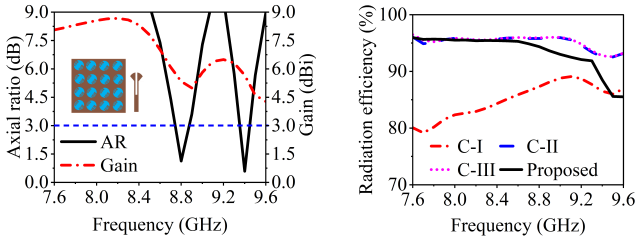

(a) (b)

Fig. 4. Simulated results of the proposed MS antenna (a) Axial ratio (dB) with gain (dBi) and (b) Radiation efficiency (%).

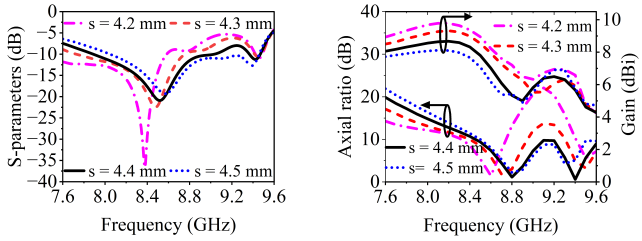

(a) (b)

Fig. 5. Simulated results of interelement spacing (s) variations (a) S-parameters (dB) (b) Axial ratio (dB) with gain (dBi).

over all the frequency ranges. By adding a radial stub with a microstrip line, the C-II obtains impedance matching below 10 dB throughout the bandwidth of (8.18–9.05 GHz) at resonance frequency 8.64 GHz. Similar to C-II, the MS antenna in C-III also attains a good IBW of 8.09–9.45 GHz at the same resonance frequency. As shown in Fig. 3(a), the proposed antenna achieves dual impedance bandwidth of 7.88–9.03 GHz and 9.36–9.46 GHz at the resonance frequencies of 8.52 GHz and 9.42 GHz by modifying the circular patch with an open rectangular slot. Fig. 3(b) displays the stepwise design's axial ratio and gain (dBi). Nevertheless, as Fig. 3(b) illustrates, the first three steps (C-I, C-II, and C-III) demonstrate that the gain is above 4.5 dB throughout frequency ranges, and the axial ratio values are 40 dB, indicating no CP performance. As seen in Fig. 3(b), the maximum gain of these three cases is greater than 8.0 dBi at 8.2 GHz. Figure 4(a) shows that the proposed antenna achieves dual circular polarization with a gain of 4.5 dBi and a 3 dB axial ratio bandwidth (8.74–8.87 GHz and 9.35–9.44 GHz.). Also, the proposed antenna achieves a maximum gain of 8.5 dB at 8.2 GHz, respectively. Figure 4(b) displays the radiation efficiency of each case. Radiation efficiency is above 80% in the C-I and above 90% in the C-II, C-III, and the proposed cases. The radiation efficiency of the proposed antenna falls at the higher frequency where the antenna operates as circularly polarized.

B. Parametric Analysis

A detailed parametric analysis of element spacing was carried out, as seen in Fig. 5. Fig. 5(a) and (b) illustrate whether spacing varies the S-parameter and axial ratio with gain. Fig. 5 shows that the impedance bandwidth increses as

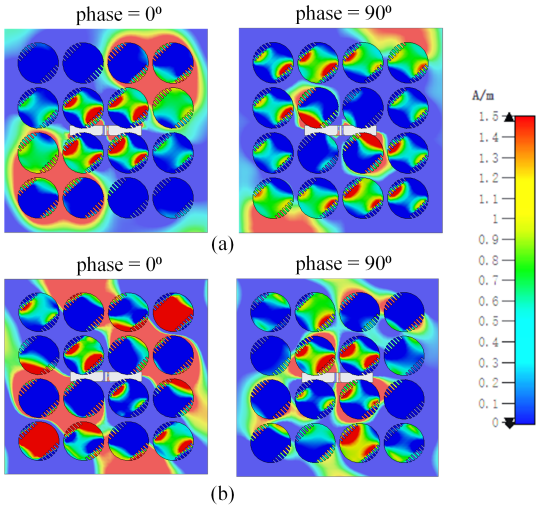

Fig. 6. Surface current distributions of an antenna element at the phase of 0° and 90° (a) 8.4 GHz and (b) 9.4 GHz.

TABLE II
COMPARISON OF THE PROPOSED ANTENNA WITH PREVIOUS WORK

Refs.	IBW(%)	Gain(dBi)	Polarization	Size ($\lambda_0{}^3$)
[5]	11.6	4.33	CP	1.41×1.41×0.05
[6]	7.8	8.5	CP	1.15×1.15×0.12
[7]	31	9.3, 4.2	LP	1.15×1.15×0.12
This work	13.6, 1.06	8.6	CP	1.15×1.15×0.047

the spacing value (s) increases. As seen in Fig. 5(b), the dual-band axial ratio is obtained at "s" = 4.4 mm, and the gain increases as "s" value decreases. The value of "s" for the dual-band CP is selected to be 4.4 mm.

C. Surface Current Distribution

The surface current distribution of the proposed MS antenna is discussed in this section. The current distribution of the MS antenna elements with phases of 0° and 90°, at 8.4 GHz and 9.4 GHz are displayed in Fig. 6(a) and (b). The patch distribution or flow of current provides information regarding the rate of electron flow relative to specified structure. Compared to other studies [5]–[7] that are highlighted in the table, the proposed design in this work possesses competitive features.

D. Radiation Patterns

Fig. 7 shows the normalized simulated left-handed circularly polarized (LHCP) and right-handed circularly polarized (RHCP) radiation patterns plots of the MS antenna at 8.8 GHz and 9.4 GHz, respectively. These radiation patterns are observed at phases of 0° and 90°.

III. CONCLUSION

To improve the impedance bandwidth of the proposed MS-based CP antenna, an open circuit radial stub termination embedded with a microstrip fed-line is presented. The MS is composed of 4 × 4 circular radiator by inserting a 45° rectangular slot to achieve dual-band CP radiation. Furthermore, the design produced LHCP and RHCP radiation with an efficiency

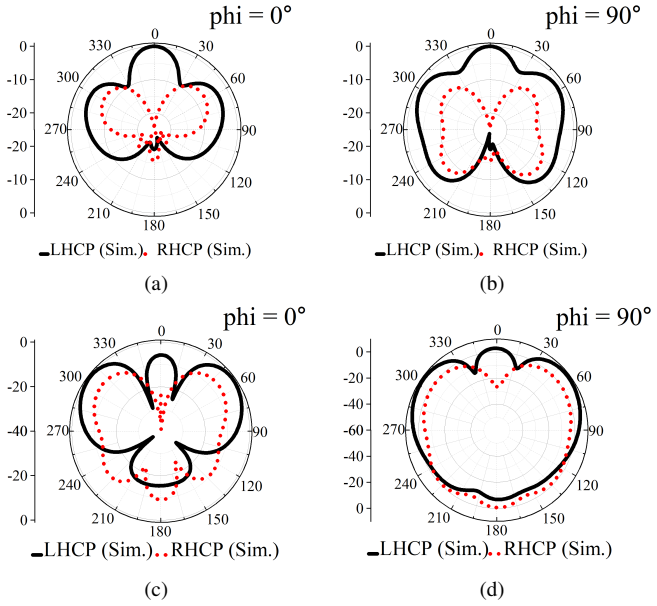

Fig. 7. Simulated results of LHCP and RHCP radiation patterns (a) (b) at 8.8 GHz (c) (d) at 9.4 GHz.

of over 90% and a gain of over 8.6 dBi at 8.2 GHz. The proposed array is a good preference for X-band applications because of its promising qualities, which include a wide and narrow operating frequency, a stable radiation pattern, high gain, and good radiation efficiency.

ACKNOWLEDGMENT

This work is supported by National Key Research and Development Program of China under Grant 2023YFE0107900, in part by the National Natural Science Foundation of China under Grant 62071306, and in part by Shenzhen Science and Technology Program under Grants JSGG20210802154203011, JCYJ20200109113601723 and JSGG20210420091805014.

REFERENCES

[1] M. Ameen, o. Ahmad and R. K. Chaudhary, "Wideband circularly polarised high-gain diversity antenna loaded with metasurface reflector for small satellite applications" Electron. Lett, vol. 55, no. 15, pp. 829–831, Jul. 2019.
[2] W. Liu, Z. N. Chen, and X. Qing, "Miniaturized broadband meta- surface antenna using stepped impedance resonators," in Proc. IEEE 5th Asia-Pacic Conf. Antennas Propag. (APCAP), pp. 365–366, Feb. 2016.
[3] S.-J. Park, D.-H. Shin, and S.-O. Park, "A low profile single dipole antenna radiating circularly polarized waves," IEEE Trans. Antennas Propag., vol. 53, no. 9, pp. 3083–3086, Sep. 2005.
[4] A. Khan, Y. He and Z. N. Chen, "A metamaterial-based broadband circularly polarized aperture-fed grid-slotted patch antenna," in Proc. IEEE 4th AsiaPacic Conf. Antennas Propag. (APCAP), pp. 353–354, Jul. 2015.
[5] P. Gao and F. Xu, "A Low-Profile Broadband Circularly Polarized Pattern Diversity Metasurface-Inspired Antenna," IEEE Trans. Antennas Propag., vol. 71, no. 10, pp. 8308–8313, Oct. 2023.
[6] W. Lin, H. Wong and R. W. Ziolkowski, "Circularly Polarized Antenna With Reconfigurable Broadside and Conical Beams Facilitated by a Mode Switchable Feed Network,," IEEE Trans. Antennas Propag., vol. 66, no. 2, pp. 996–1001, Feb. 2018.
[7] C. Deng, X. Lv and Z. Feng, "Wideband Dual-Mode Patch Antenna With Compact CPW Feeding Network for Pattern Diversity Application," IEEE Trans. Antennas Propag., vol. 66, no. 5, pp. 2628–2633, May. 2018.